Available online at www.sciencedirect.com
SCIENCE DIRECT®
Sensors and Actuators B 104 (2005) 124–131
SENSORS AND ACTUATORS B CHEMICAL
www.elsevier.com/locate/snb

Ethanol and H_2S gas detection in air and in reducing and oxidising ambience: application of pattern recognition to analyse the output from temperature-modulated nanoparticulate WO_3 gas sensors

R. Ionescu [a,b,*], A. Hoel [a], C.G. Granqvist [a], E. Llobet [b], P. Heszler [a,1]

[a] *The Ångström Laboratory, Department of Engineering Sciences, Uppsala University, P.O. Box 534, SE-75121 Uppsala, Sweden*
[b] *Department of Electronics, Electrical and Automation Engineering, Rovira i Virgili University, Avenue Paisos Catalans 26, ES-43007 Tarragona, Spain*

Received 9 March 2004; received in revised form 30 April 2004; accepted 10 May 2004
Available online 2 September 2004

Abstract

Ethanol and H_2S, mixed with air or NO_2, were detected using a novel nanocrystalline WO_3 sensor produced by advanced gas deposition and operated in a dynamic mode effected by square voltage pulses applied to its heating element, thereby modulating the operating temperature between 150 and 250 °C. The sensor signals were decomposed by fast Fourier and discrete wavelet transforms, and the ensuing data were used as inputs into various pattern recognition methods for identification and quantification purposes. We were able to show that ethanol and H_2S could be detected with good sensitivity and selectivity in the presence of both reducing and oxidizing gases.

Keywords: Gas sensor; Temperature modulation; Fast Fourier transform analysis; Wavelet analysis; Pattern recognition; Tungsten oxide; Nanoparticle

1. Introduction

Even though the olfactory system of humans is exceptional at detecting and identifying many odours, most hazardous gases or vapours can only be recorded at too high concentrations or cannot be detected at all. Standardised methods for ambient air determination involve the use of various techniques and technologies as well as expensive and bulky equipment. All of the methods require laboratory procedures incapable of obtaining real-time results. However, serious attempts to control pollution demand that emissions of hazardous gases into the atmosphere be continuously monitored. Classical analytical methods are not suitable for such real-time analysis, and it follows that there is a need for developing rugged, reliable, small, and inexpensive equipment for air quality monitoring.

Metal-oxide semiconductor gas sensors represent one option for constructing gas monitors. They operate on the principle that the sensor's resistance changes in the presence of reducing or oxidising gases [1]. Although the analysis of single gases and multi-component mixtures by using metal-oxide-based semiconductor gas sensors has been the subject of research for more than 20 years, a number of problems associated with this approach remain unsolved. For example, it is well known that metal-oxide-based gas sensors suffer from drift and lack of selectivity [2], which explains why they are presently used only in low-cost, alarm-level gas monitors for domestic and industrial application [3].

The limited selectivity of semiconductor gas sensors can be evaded in several ways, and a number of different strategies—all having been applied with limited success have been reported. A recent approach consists of analysing the sensor's dynamic response in order to obtain a new set of parameters specific to the investigated gases, one easily implemented method being based on changes in the operating temperature for generating suitable response transients [4]. The required modulation can be obtained by applying a variable signal to a heating element in contact with the sensor. The objective of the temperature modulation is then to alter the kinetics of adsorption and desorption reactions that occur at the sensor's surface in the presence of gaseous species. Previous work of this kind has shown that a modulation of the sensor's working temperature leads to

* Corresponding author. Tel.: +34 977 55 87 64; fax: +34 977 55 96 05.
E-mail address: rionescu@etse.urv.es (R. Ionescu).
[1] Research Group on Laser Physics of the Hungarian Academy of Sciences, University of Szeged, P.O.Box 406, H-6701 Szeged, Hungary

0925-4005/$ – see front matter © 2004 Elsevier B.V. All rights reserved.
doi:10.1016/j.snb.2004.05.014

a response pattern that is characteristic for the gas under investigation [5–8].

The most commonly used method to extract important features from response signals of temperature-modulated gas sensors is the fast Fourier transform (FFT). An alternative way for decomposing a signal into its constituent parts is the discrete wavelet transform (DWT). The main difference between the two methods is that DWT provides both frequency and temporal information of the signal, while FFT gives only frequency information for the complete duration of the signal so that the temporal information is lost. The ensuing data are used as inputs into various pattern recognition methods for identification and quantification purposes.

The FFT and DWT coefficients provide 'fingerprints' that are characteristic of the concentration level and gas measured. They depend on the chemical reactions that take place between the active film of the sensor and the gas and are, thereby, directly influenced by the characteristics of the active material used and its deposition method. Thus, another important requirement for enhancing the selectivity is the availability of very accurately controlled preparation techniques for the sensor material. Such techniques should be able to provide the desired oxide composition at a minimum number of processing steps. In practice, selectivity is achieved by enhancing gas adsorption or promoting specific chemical reactions via catalytic or electronic effects using bulk dopants, surface modification methods, or by addition of metallic clusters or oxide catalysts [9,10].

In general, sensitivity is improved by microstructural changes such as the reduction of the oxide particle size to the nanometre scale [11] and nanostructured materials are recognised as essential for achieving high gas sensitivity. These materials present new opportunities for enhancing the performance of gas sensors as a consequence of their large surface area and because a significant fraction of their atoms reside at grain boundaries [12,13]. Prior work has shown that the sensitivity of semiconductor oxide materials has been improved by reducing the particle size, and greatly improved properties have been reported for sizes in the 5–50 nm range [14,15].

In the present paper, we detect ethanol and H_2S mixed with dry air or NO_2 using a novel nanocrystalline WO_3 sensor (thickens about 20 μm) produced by advanced gas deposition. The sensor was operated in the dynamic mode effected by square voltage pulses applied to its heating element, thus modulating its temperature between 150 and 250 °C. The sensor signals were decomposed by the FFT and DWT transforms, and the features extracted were used as inputs into various pattern recognition methods for identification and quantification purposes. In particular, unsupervised and supervised pattern recognition methods, specifically principal component analysis (PCA) and discriminant factor analysis (DFA), as well as neuronal networks, specifically fuzzy ARTMAP and radial basis functions (RBF), were applied to distinguish the investigated gases. Furthermore, a linear multivariate statistical algorithm, specifically partial least squares (PLS), was used to build predictive models for ethanol and H_2S concentrations both for pure and mixed gases, and fuzzy ARTMAP and RBF neural networks were also implemented for identifying the class of concentration to which each measurement belonged. The results obtained have shown that ethanol and H_2S gases can be detected with good sensitivity and selectivity in the presence of both reducing and oxidising species.

2. Experimental

WO_3 nanoparticle thick-film gas sensors were employed for the measurements. The sensor device comprised an alumina substrate (9 mm × 7 mm) with two pre-printed gold electrodes, 0.3 mm apart and 5 mm in length, on the upper side and a Pt heating resistor on the reverse side [16]. The WO_3 nanoparticle film was deposited onto the substrate by using an advanced gas deposition unit (ultra fine particle equipment, ULVAC Ltd., Japan). Further details on this apparatus and on the deposition process can be found elsewhere [17,18]. The deposited film was annealed at 600 °C in air, exhibiting then a monoclinic phase with an average grain size of about 23 nm [17,19]. The WO_3 film was 20 μm thick.

The measurement set-up comprised of a 300 ml test chamber, three mass-flow controllers, and a data acquisition system for recordings in the millisecond range, employed for acquiring the sensor's resistance. The temperature of the sensor was varied between 150 and 250 °C by applying square voltage pulses with a frequency of 36 mHz to its heating resistor. The temperature range and the frequency were optimised for the analysed gases. Synthetic dry air (80% N_2 and 20% O_2) at a constant flow rate of 1 l/min was used as both purging and carrier gas.

The sensor was exposed to controlled concentrations of ethanol (10, 50, and 100 ppm), H_2S (1, 5, and 10 ppm), ethanol + H_2S (10 + 1, 50 + 5, and 100 + 10 ppm), ethanol + NO_2 (10 + 1, 50 + 5, and 100 + 10 ppm), and H_2S + NO_2 (1 + 1, 5 + 5, and 10 + 10 ppm). All concentrations were diluted in dry air. Each measurement was replicated four times in order to obtain representative data. Data acquisition started 3 min before the injection of a gas sample into the airflow and took 20 min to complete. The sampling rate was set to 1.33 s^{-1}, i.e. new data was stored every 0.6 s. For purging of the measurement chamber, each measurement was followed by a temperature treatment at 300 °C for 15 min, and subsequently the sensor, subjected to the voltage pulses, was kept for 1 h in the presence of synthetic dry air for recuperating its baseline resistance.

3. Results and discussion

For assessing the selectivity of the WO_3 nanoparticle gas sensor employed in the measurements, the acquired data

were divided into two subsets (denoted A and B), which were formed so that the detection of a single gas in air and in the presence of reducing and oxidising species followed in suite. The two subsets were as follows.

- A: ethanol; ethanol + H_2S (i.e. reducing species); ethanol + NO_2 (i.e. oxidising species)
- B: H_2S; H_2S + ethanol (i.e. reducing species); H_2S + NO_2 (i.e. oxidising species)

The same measurements for ethanol + H_2S were used in both subsets.

In order to extract important parameters characteristic of the studied gases, the sensor signals were first decomposed by either a FFT or a DWT technique.

A 540-sample (comprising 20 periods of the sensor response) FFT was performed for every response transient. The transform works by first translating a function in the time domain into a function in the frequency domain. The signal can then be analysed for its frequency content because the Fourier coefficients of the transformed function represent the contribution of each sine and cosine function at each frequency. The amplitude of the dc component and the first three harmonics of the FFT were extracted. FFT coefficients of the higher harmonics were discarded because they had very low amplitudes, and low amplitude harmonics corresponding to high frequencies may be affected by noise. The FFT had to be calculated over a sufficiently large number of samples to provide a good definition of the harmonic peaks.

The DWT was computed over a single period of the sensor response (28 samples) chosen soon after the introduction of the test gas into the measurement chamber. Only one period suffices to compute the DWT because a DWT decomposition presents very similar features, periodically distributed for the different time positions, when a large number of periods is considered [20].

DWT uses a windowing technique with regions of different sizes, allowing long-duration windows to be used for accurate low-frequency information combined with short-duration windows for accurate high-frequency information. Wavelet scale refers to the width of the window; as the scale is increased, more coefficients are used to define the analysed sequence of data and a finer level of detail is obtained [21]. Specifically, the Daubechies family of wavelets was used for the analysis because of its desirable properties of orthogonality, approximation quality, redundancy and numerical stability [22]. In particular, the fourth order Daubechies (db4) was considered convenient as it is the first 'smooth' wavelet of the family, and a level-3 decomposition of the sensor response was performed. The wavelet coefficients from 5 to 16, corresponding to the wavelets of scales 2 and 3, were selected for further analysis. DWT coefficients between 1 and 4 were discarded because they correspond to very low frequencies and are affected by drift [8]. Higher DWT coefficients than the 16th were not selected because they correspond to high frequencies in the response signals and may be affected by noise [20].

The data matrices formed either with the FFT or DWT coefficients were then used as inputs into different pattern recognition methods in order to classify and quantify the measured gases.

3.1. Sensitivity curves

Sensitivity curves for ethanol-based measurements (subset A) and H_2S-based measurements (subset B) were studied initially. The sensitivity (S) was defined as the ratio between the variation of the sensor resistance in air (ΔR_{air}) and the variation of the sensor resistance 15 min after the exposure to the test gas (ΔR_{gas}) according to:

$$S = \frac{\Delta R_{air}}{\Delta R_{gas}} \quad (1)$$

where ΔR represents the difference between the maximum and minimum values of the sensor resistance during one complete period of thermal cycling.

Table 1 summarises mean values for the sensitivity of the four replicate measurements at each gas concentration (x) and the linear dependence between S and x. The columns in the table are arranged for increasing concentration of the gases. As expected, the sensitivity was higher for a mixture of two reducing gases than for only one reducing gas. It was also found that the sensitivity was higher for a mixture of a reducing and an oxidising species than for the reducing gas only. This is counter to the expected behaviour for the sensor in the presence of an oxidising species for which case

Table 1
Mean values for sensor sensitivity (S) upon exposure to various pure gases and gas mixtures, and functional relationship between sensitivity and gas concentration (x)

Gas	Mean value for sensitivity			Sensitivity dependence on concentration
	Lowest concentration	Medium concentration	Highest concentration	
Ethanol	7.3	48.2	76.4	$S = 0.76x + 3.5$
Ethanol + H_2S	16.7	141.6	328.3	$S = 3.5x - 23$
Ethanol + NO_2	64.8	132.2	208.5	$S = 1.6x + 50$
H_2S	5.6	42.1	82.5	$S = 8.5x - 2.1$
H_2S + ethanol	16.7	141.6	328.3	$S = 35x - 23$
H_2S + NO_2	4.5	55.8	144.4	$S = 16x - 15$

the resistance should increase, and thus the sensitivity of the sensor in contact with the oxidising and reducing species should decrease. Nevertheless, the observed result may be reconciled with the highly complex behaviour that NO_2 was found to exhibit as a function of the surface temperature of the sensor [23].

3.2. Qualitative analysis

Qualitative analyses were performed for the gases belonging to subsets A and B with the aim to discriminate between the reducing gas, the mixture of the two reducing gases, and the mixture of the reducing and the oxidising gases.

A linear unsupervised method was first applied. To this end, a PCA was performed using either the selected FFT or DWT coefficients. The objective of PCA is to express the information from the variables of the response matrix by a lower number of variables called principal components (PCs) [24]. The PCs are chosen to contain the maximum variance in the data and to be orthogonal. The response matrix is decomposed into a product of two matrices (scores and loadings). While the loadings matrix contains the contribution of the original response vectors to the new response vectors or PCs, the score matrix contains the response vectors projected onto the space defined by the PCs.

Figs. 1 and 2 show score plots of the PCA for the pure gases and gas mixtures belonging to subsets A and B, respectively, with FFT (upper panels) and DWT (lower panels) used as feature extractors. The data matrices were mean-centred, and the first two principal components accounted for more than 99.9% of the variance in all of the considered cases.

For subset A, the ethanol + NO_2 measurements were well separated from data emanating from the other two classes when the DWT coefficients were used (Fig. 1, lower panel) and the separation was rather good also when the FFT coefficients were employed (Fig. 1, upper panel). On the other hand, a grouping of the measurements on ethanol and on ethanol + H_2S was not possible. Anyway, a careful study of the PCA plot can conclude that the first principal component had negative scores for measurements containing 10 ppm of ethanol, and positive scores for measurements containing 50 or 100 ppm of ethanol. Another important remark is that the measurements within each class were arranged in order of increasing gas concentration, i.e. in the sense indicated by the arrows. This implies that the FFT and DWT coefficients are concentration-dependent and could be employed to perform quantitative analyses.

For subset B, the measurements could not be classified at all when FFT coefficients were used (Fig. 2, upper panel). When the DWT coefficients were used, however, the H_2S + ethanol measurements were well separated from data emanating from the other two classes (Fig. 2, lower panel). Again the measurements were arranged according to increasing gas concentration, and it is apparent that quantitative analyses are feasible. Although it is not as clear as when the DWT was used, favourable concentration dependence was found also when the FFT coefficients were used.

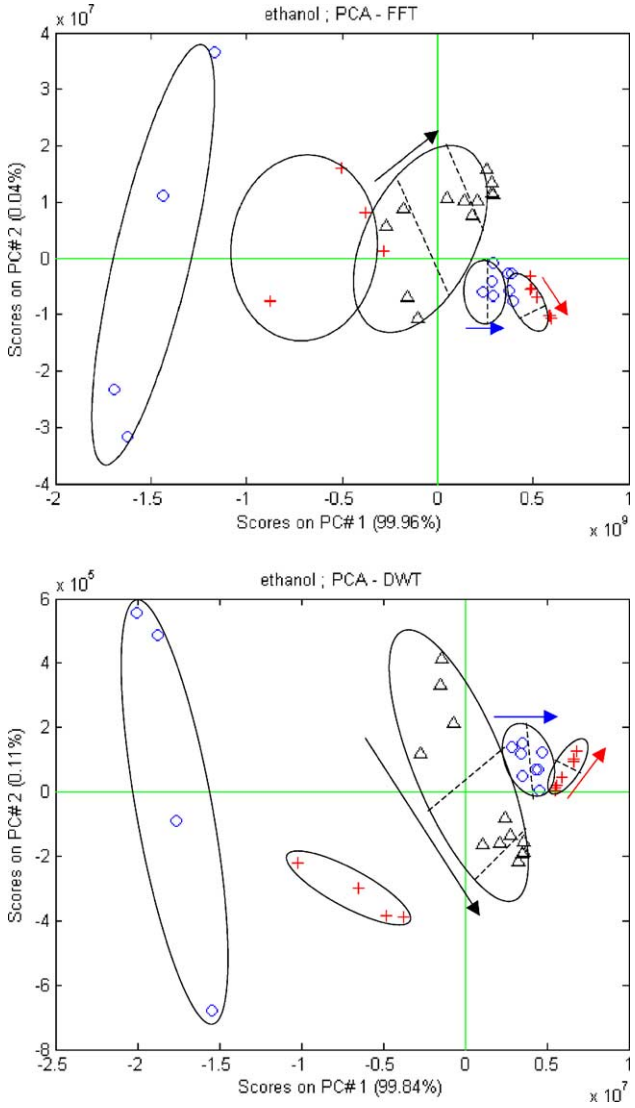

Fig. 1. Principal components analysis applied to ethanol-containing gases (i.e. subset A) using fast Fourier transform coefficients (upper panel) and discrete wavelet transform coefficients (lower panel). Data refer to ethanol (◇), ethanol + H_2S (+), and ethanol + NO_2 (△). Arrows indicate increasing gas concentrations.

The analysis based on PCA showed that the investigated gases, in general, could not be well discriminated. In order to improve on this situation, a 3-class DFA, a linear supervised method which was also invoked. The three pre-defined classes were the single gas, the mixture of the two reducing gases, and the mixture of the reducing and the oxidising gases. Like PCA, DFA finds new orthogonal axes (factors) as a linear combination of the input variables. Unlike PCA, however, DFA computes the factors as to minimise the variance within each class and maximise the variance between classes [25]. The data matrices were the same as those used for the PCA.

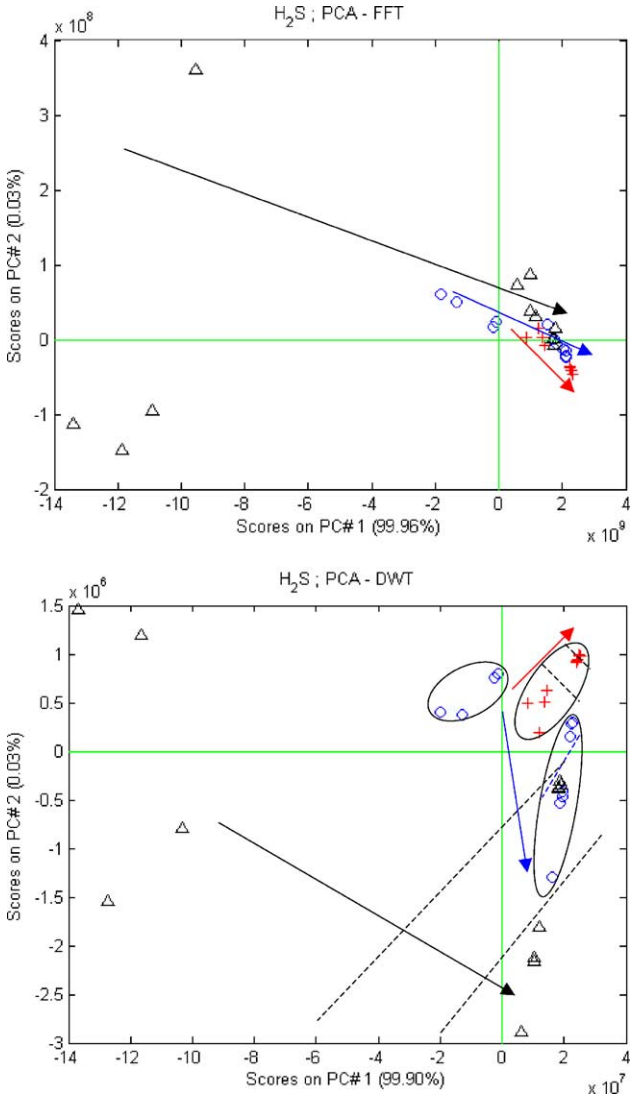

Fig. 2. Principal components analysis applied to H_2S-containing gases (i.e. subset B) using fast Fourier transform coefficients (upper panel) and discrete wavelet transform coefficients (lower panel). Data refer to H_2S (○), H_2S + ethanol (+), and H_2S + NO_2 (△). Arrows indicate increasing gas concentrations.

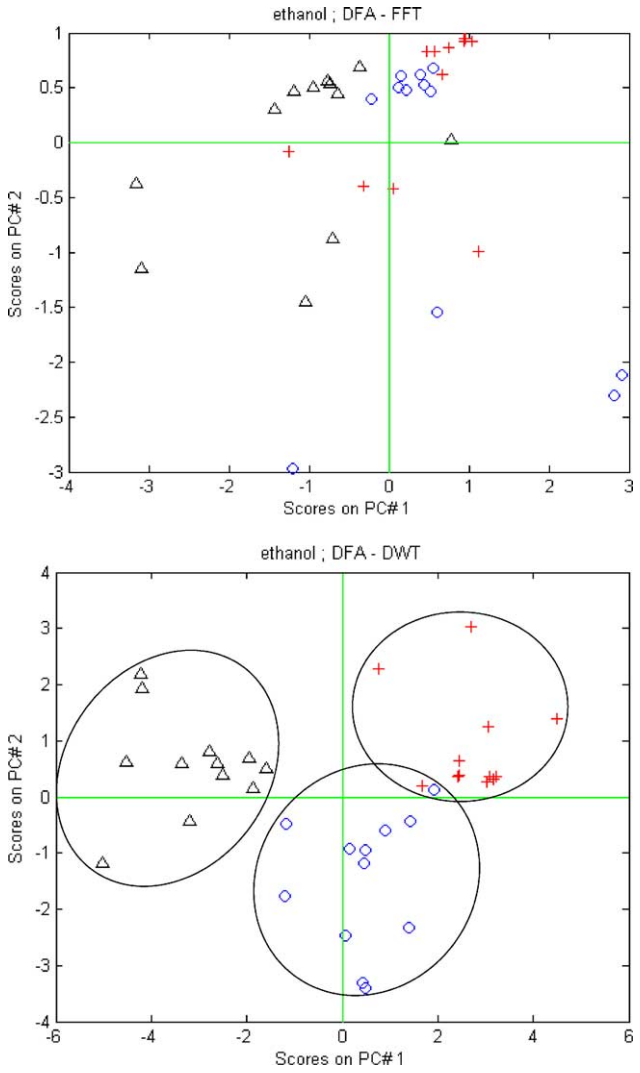

Fig. 3. A 3-class discriminant factorial analysis applied to ethanol-containing gases (i.e. subset A) using fast Fourier transform coefficients (upper panel) and discrete wavelet transform coefficients (lower panel). Data refer to ethanol (○), ethanol + H_2S (+), and ethanol + NO_2 (△).

Figs. 3 and 4 show score plots of the DFA for the pure gases and gas mixtures belonging to subsets A and B, respectively, with FFT (upper panels) or DWT (lower panels) used as feature extractors. For the ethanol-containing gases (subset A), a fairly good separation between the three classes was obtained when the DWT coefficients were used (Fig. 3, lower panel). When the FFT coefficients were used, a classification of the gas species was not possible (Fig. 3, upper panel). For H_2S-containing gases (subset B), three very distinct clusters of data points were formed for the various gases when the DWT coefficients were employed (Fig. 4, lower panel). Again, the discrimination between the gases was not possible when the FFT coefficients were applied (Fig. 4, upper panel).

Finally, two non-linear pattern recognition methods were tested for qualitative analyses of the pure and mixed gases. A neural network has a specific architecture and uses specific algorithms for training. During the training phase, it continuously adapts its intern structure so that to better approximate the final conditions. Once trained, it provides information on any new measurement projected onto its structure.

A fuzzy ARTMAP neural network [26,27] and a RBF neural network [28] were employed for this study. The implemented networks had their number of input neurons equal to the numbers of selected FFT or DWT coefficients (4 or 12, respectively). The number of output neurons was set to three since a one-of-three code was used to code the three different categories that formed one subset of data. Because of the limited number of measurements available for each subset of data (specifically being 36), a leave-one-out cross-validation method was used to estimate the success rate of the networks. Given the 36 measurements, the networks were trained 36

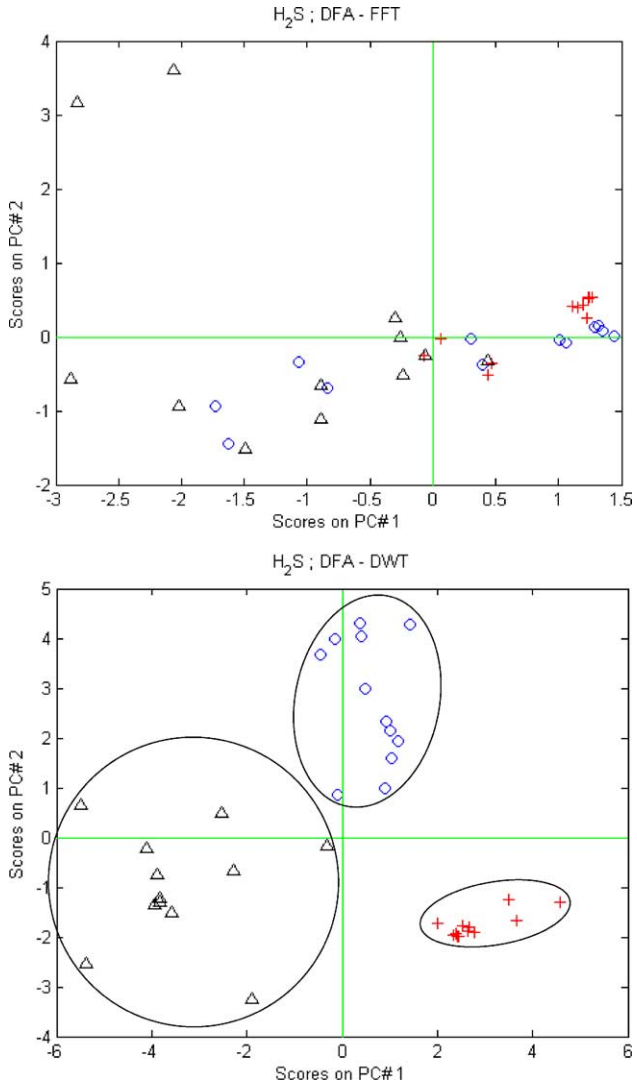

Fig. 4. A 3-class discriminant factorial analysis applied to H_2S-containing gases (i.e. subset B) using fast Fourier transform coefficients (upper panel) and discrete wavelet transform coefficients (lower panel). Data refer to H_2S (○), H_2S + ethanol (+), and $H_2S + NO_2$ (△).

times, using 35 training vectors. The vector left out during the training phase was then used for testing.

When fuzzy ARTMAP was employed, the coefficient matrices were either column or globally normalised, as this network requires inputs in the range 0–1. By applying a column-normalisation, the intensity between the different columns in the matrix is lost as each column is divided by its maximum. When a global normalisation is performed, the elements in the matrix are divided by the maximum of the matrix, so then the differences between columns are kept. The performance of the networks, calculated as the average performance over the 36 tests, is shown in Table 2. The gas species from subset A (i.e. ethanol-containing gases) were better classified than the ones from subset B (H_2S-containing gases). For all studied cases, the use of DWT coefficients led to a better classification than the use of FFT coefficients. However, the best results were obtained with the fuzzy ARTMAP neural network. When the matrix of DWT coefficients was column-normalised, fuzzy ARTMAP correctly predicted the class of all the available ethanol-based measurements.

Table 2
Classification success rate using fuzzy ARTMAP and RBF neural networks

	Neural network	Normalisation	FFT coefficient (%)	DWT coefficient (%)
Subset A	fuzzy ARTMAP	Column	80.6	100
		Global	83.3	94.4
	RBF	–	80.6	94.4
Subset B	fuzzy ARTMAP	Column	80.6	91.7
		Global	77.8	83.3
	RBF	–	66.7	80.6

Three classes of gas species were defined for each subset of data. The data are based on FFT and DWT analyses.

3.3. Quantitative analysis

Finally, a quantitative analysis of the gases was attempted. A PLS method—which is a linear multivariate statistical algorithm—was used initially to build predictive models for ethanol and H_2S concentrations, both for pure and mixed gases. PLS is a supervised calibration method that captures as much variance as possible in the predictor block (i.e. response matrix), under the constrain of being correlated with the predicted block (i.e. concentration matrix) [29]. The matrices of input data with the FFT or DWT coefficients were mean-centred. As only a few measurements per category were available (specifically 12), the prediction of gas concentration was evaluated using a leave-one-out cross-validation method. Thus a model was built 12 times using 11 measurements, and the remaining one was used for testing.

Two methods were employed to compare the concentrations predicted by the PLS models with experimental ones. First, correlation coefficients between real and predicted gas concentrations were calculated. A superior prediction is signified by the coefficients being close to unity. Then a linear fitting was calculated between the real and predicted concentrations. A perfect prediction would yield unity slope and zero intercept. The results of this analysis, summarised in Table 3, show that very good predictions were obtained when the DWT coefficients were employed.

A fuzzy ARTMAP neural network and an RBF neural network were then implemented for identifying the class of concentration to which each measurement belonged. To this end, nine classes were defined for each subset of data, corresponding to increasing concentrations of each gas in the subset. The input matrix was formed by either the FFT or DWT coefficients, and it was normalised (either by column or globally) before training the fuzzy ARTMAP neural network. The leave-one-out cross-validation method was again used for estimating the performance of the networks.

Table 3
Summary of results for quantitative gas analyses using PLS models

	Coefficient used	Number of LV	Correlation coefficient	Slope	Intercept (ppm)
Ethanol	FFT	2	0.8447	0.7280	14.2839
	DWT	8	0.8685	0.9029	3.8130
Ethanol + H_2S	FFT	2	0.8302	0.7920	10.2964
	DWT	7	0.9438	0.9911	1.5845
Ethanol + NO_2	FFT	2	0.9221	0.8892	4.9005
	DWT	10	0.9950	0.9936	−0.4527
H_2S	FFT	4	0.8774	0.9612	−0.3160
	DWT	10	0.9956	0.9689	0.0906
H_2S + ethanol	FFT	2	0.8302	0.7920	1.0296
	DWT	7	0.9438	0.9911	0.1584
H_2S + NO_2	FFT	4	0.8370	1.0063	−0.6779
	DWT	10	0.9769	0.9688	0.0758

LV denotes latent variable.

Table 4
Quantification success rate for ethanol-containing and H_2S-containing gases obtained with fuzzy ARTMAP and RBF neural networks

	Neural network	Normalisation	FFT coefficient (%)	DWT coefficient (%)
Subset A	fuzzy ARTMAP	Column	80.6	94.4
		Global	80.6	94.4
	RBF	–	69.4	91.7
Subset B	fuzzy ARTMAP	Column	77.8	83.3
		Global	66.7	77.8
	RBF	–	63.9	72.2

The 9-class concentration levels were defined for each subset of data. The data are based on FFT and DWT analyses.

The performance of the networks, calculated as the average performance over the 36 tests, is given in Table 4. Superior results were obtained when the DWT coefficients were used in the analyses, and again fuzzy ARTMAP led to better predictions than RBF. The success rate was higher for the ethanol-containing gases (subset A). In this case, only two measurements out of 36 were misclassified when the fuzzy ARTMAP neural network was employed and the DWT coefficients were used, no matter what kind of normalisation was performed. On the other hand, for the ethanol-containing gases (subset A), similar results were obtained when the data were column or globally normalised before introducing them into the fuzzy ARTMAP network, while the column-normalisation gave better results for the H_2S-containing gases (subset B).

4. Conclusions

Nanoparticle films of crystalline WO_3 were deposited onto alumina substrates by reactive gas deposition and were employed for gas sensing applications. H_2S, ethanol vapour, and binary mixtures of ethanol + H_2S, ethanol + NO_2, and H_2S + NO_2 were used in different concentrations in air for testing the performance of the sensor.

The sensor was operated in a dynamic mode by modulating its temperature between 150 and 250 °C. Coefficients were extracted from fast Fourier transform and discrete wavelet transform methods applied to the dynamic resistance response of the sensor. The obtained coefficients were then used as inputs into different pattern recognition methods to extract both quantitative (concentration) and qualitative (chemical selectivity) information concerning the gases.

When FFT coefficients were used in the pattern recognition the chemical classification success rate was about 80%, whereas the use of DWT coefficients resulted in an identification success rate close to 100%. The correlation coefficients between the real and predicted gas concentrations lay between 0.8302 and 0.9221 for the different pure and mixed gases analysed when FFT coefficients were used, and between 0.8685 and 0.9956 when DWT coefficients were employed. The superior results obtained with wavelet analysis can be explained by the fact that a careful selection of DWT coefficients reduces sensor drift and noise effects. The results of the present work unambiguously show the potential of the new dynamic sensor techniques, especially regarding chemical selectivity.

Acknowledgements

The authors are grateful to Dr. J. Ederth from Uppsala University (Sweden), to Mr. A. Vergara from Rovira i Virgili University of Tarragona (Spain) and to Mr. C. Duran from the University of Pamplona (Colombia) for helpful discussions. One of the authors (R. Ionescu) gratefully acknowledges a doctoral fellowship from the Rovira i Virgili University. This work has been supported by the Marie Curie Host Fellowship Program of the European Commission (contract no. HPMT-CT-2001-00307).

References

[1] M.J. Madou, S.R. Morrison, Chemical Sensing with Solid State Devices, Academic Press, San Diego, USA, 1999.
[2] P. Moseley, B. Tofield, Solid State Gas Sensors, Adam Hilger, Bristol, UK, 1987.
[3] J. Chou, Hazardous Gas Monitors, McGraw-Hill, New York, USA, 2000.
[4] W.M. Sears, K. Colbow, R. Slamka, F. Consadori, Selective thermally cycled gas sensing using fast Fourier-transform techniques, Sens. Actuators B 2 (1990) 283–289.
[5] R.E. Cavicchi, J.E. Suehle, K.G. Kreider, M. Gaitan, P. Chaparala, Optimised temperature-pulse sequences for the enhancement of chemically specific response pattern from micro-hotplate gas sensors, Sens. Actuators B 33 (1996) 142–146.
[6] E. Llobet, R. Ionescu, S. Al-Khalifa, J. Brezmes, X. Vilanova, X. Correig, N. Bârsan, J.W. Gardner, Multi component gas mixture analysis using a single tin oxide sensor and dynamic pattern recognition, IEEE Sens. J. 1 (2001) 207–213.
[7] R. Ionescu, E. Llobet, Wavelet transform-based fast feature extraction from temperature modulated semiconductor gas sensors, Sens. Actuators B 81 (2002) 289–295.
[8] E. Llobet, J. Brezmes, R. Ionescu, X. Vilanova, S. Al-Khalifa, J.W. Gardner, N. Bârsan, X. Correig, Wavelet transform and fuzzy ARTMAP-based pattern recognition for fast gas identification using a micro-hotplate gas sensor, Sens. Actuators B 83 (2002) 238–244.
[9] W. Göpel, New materials and transducers for chemical sensors, Sens. Actuators B 18–19 (1994) 1–21.
[10] V. Demarne, R. Sanjines, in: G. Sberveglieri (Ed.), Gas Sensors Principles, Operation and Development, Kluwer Academic, Dordrecht, The Netherlands, 1992, pp. 89–116.
[11] C. Xu, J. Tamaki, N. Miura, N. Yamazoe, Grain size effects on gas sensitivity of porous SnO_2-based elements, Sens. Actuators B 3 (1991) 147–155.
[12] H. Gleiter, Nanocrystalline materials, Progr. Mater. Sci. 33 (1989) 223–315.
[13] R.W. Siegel, Cluster-assembled nanophase materials, Ann. Rev. Mater. Sci. 21 (1991) 559–578.
[14] Y. Shimizu, M. Egashira, Basic aspects and challenges of semiconductor gas sensors, MRS Bull. 24 (1999) 18–24.
[15] N. Yamazoe, New approaches for improving semiconductor gas sensors, Sens. Actuators B 5 (1991) 7–19.
[16] V. Lantto, in: G. Sberveglieri (Ed.), Gas Sensors, Kluwer Academic, Dordrecht, The Netherlands, 1992.
[17] J.L. Solis, A. Hoel, L.B. Kish, C.G. Granqvist, S. Saukko, V. Lantto, Gas-sensing properties of nanocrystalline WO_3 films made by advanced reactive gas deposition, J. Am. Ceram. Soc. 84 (2001) 1504–1508.
[18] A. Hoel, L.K.J. Vandamme, L.B. Kish, E. Olsson, Current and voltage noise in WO_3 nanoparticle films, J. Appl. Phys. 91 (2002) 5221–5226.
[19] A. Hoel, L.B. Kish, R. Vajtai, G.A. Niklasson, C.G. Granqvist, E. Olsson, Electrical properties of nanocrystalline tungsten trioxide, Proc. MRS 581 (2000) 15–20.
[20] R. Ionescu, E. Llobet, X. Vilanova, J. Brezmes, J.E. Sueiras, J. Calderer, X. Correig, Quantitative analysis of NO_2 in the presence of CO using a single tungsten oxide semiconductor sensor and dynamic signal processing, The Analyst 127 (2002) 1237–1246.
[21] C. Torrence, G.P. Compo, A practical guide to wavelet analysis, http://paos.colorado.edu/research/wavelets.
[22] I. Daubechies, Orthogonal basis of compactly supported wavelets, Commun. Pure Appl. Math. 41 (1998) 909–996.
[23] B. Ruhland, T. Becker, G. Müller, Gas–kinetic interactions of nitrous oxides with SnO_2 surfaces, Sens. Actuators B 50 (1998) 85–94.
[24] L.T. Joliffe, Principal Component Analysis, Springer Verlag, NY, USA, 1986.
[25] R.G. Brereton, Chemometrics, Application of Mathematics and Statistics to Laboratory Systems, Ellis Horwood, Chichester, UK, 1990.
[26] G. Carpenter, S. Grossberg, N. Markuzon, J. Reynolds, D. Rosen, fuzzy ARTMAP: A neural network architecture for incremental supervised learning of analog multidimensional maps, IEEE Trans. Neural Networks 3 (5) (1992) 698–713.
[27] G. Carpenter, S. Grossberg, J. Reynolds, A fuzzy ARTMAP nanoparametric probability estimator for non-stationary pattern recognition problems, IEEE Trans. Neural networks 6 (6) (1995) 1330–1336.
[28] C.M. Bishop, Neural Networks for Pattern Recognition, Oxford University Press, Oxford, UK, 1995 (Chapter 5).
[29] P. Geladi, B.R. Kowalski, Partial least-squares regression: a tutorial, Anal. Chim. Acta 185 (1986) 1–17.